Fully distributed security constrained optimal power flow with primary frequency control

Maxime Velay, Meritxell Vinyals, Yvon Besanger, Nicolas Retière

Fully distributed security constrained optimal power flow with primary frequency control[☆]

M. Velay[a,b], M. Vinyals[a], Y. Besanger[b], N. Retiere[b]

[a] *CEA, LIST, Laboratoire d'Analyse des Données et d'Intelligence des Systèmes, Gif-sur-Yvette, 91191 France*
[b] *Univ. Grenoble Alpes, CNRS, Grenoble INP [0] , G2Elab, 38000 Grenoble, France*

Abstract

Primary frequency control is the automatic mechanism implemented on power systems to regulate the power balance through frequency and hence, its action should be taken into account when modeling any contingency state leading to a modification of the active power balance (e.g. generator failures). This paper presents a fully distributed method to solve the DC security constrained power flow (DC-SCOPF) that takes into account the automatic primary frequency response of generators after an incident. In more detail, we extend existing distributed DC-SCOPF formulations by: (1) introducing a new variable representing the frequency deviation; and (2) enhancing the local problem of each generator to consider how it adjusts its production after each contingency following its primary frequency regulation curve. The computation of the frequency deviations in the DC-SCOPF problem is formulated into a suitable form (i.e. in the form of a general consensus problem) so that smaller problems, corresponding to individual sub-regions or actors, can be solved and coordinated via the alternating direction method of multipliers (ADMM) in a distributed manner. In this way, actors of the system do not need to exchange any confidential information with other actors during the optimization procedure. A salient feature of our approach is that it can consider contingencies that lead to area separation without any prior specification of the topology and thus can adapt to many kinds of situations that are of interest in interconnected systems. Extensive simulation results on several standard IEEE systems show the good performance of the proposed model and algorithm in terms of convergence speed and accuracy as well as its capacity to deal with the disconnection of areas in interconnected systems.

Keywords: Distributed optimization, Distributed Security-Constrained Optimal Power Flow, Primary Frequency Control, Alternating Direction Method of Multipliers, Power System Interconnection

1. Introduction

The planning and operation of power systems is one of the more challenging problems faced by transmission system operators (TSOs) given the complex interplay of the multiple economic and reliability objectives to be achieved. On one side, electricity is a commodity that cannot be easily stored, so TSOs need to keep the balance between generation and consumption while minimizing the system operating cost and enforcing the network's operational constraints (e.g. the capacity of the transmission lines) during each operating period. On the other side, TSOs need to perform contingency analysis to guarantee not only that no operational constraint is violated during the normal operating case, but also after any credible contingency[1] occurs.

Therefore, to find a secure generation dispatch, each TSO requires to solve on a daily basis the so-called Security Constrained Optimal Power Flow (SCOPF) [2], an extension of the OPF problem [3] that takes into account constraints arising from the operation of the system under a set of pre-defined contingencies. The set of considered contingencies depends on the selected reliability criterion but most of the TSOs must operate at least in compliance with the N-1 criterion so that any *single* major element contingency (i.e. involving the failure of at most one system component) can be handled, leading to a stable operating point, i.e., with no propagation of the disturbance [4]. Modeling the propagation of the disturbance requires to consider the automatic actions that take place as a result of a contingency (e.g. automatic tap-changers, automatic frequency control schemes, ...). In particular, when the disturbance results in imbalances between production and consumption, it is crucial to model the primary frequency responses of generators that automatically[2] change their scheduled active production to quickly[3] restore the power balance [5]. Under these primary frequency control schemes, the generating units use the frequency to regulate the power supplied since it reflects the power balance in the system. SCOPF problems considering these automatic reactions of the system are called *preventive*, as opposed to *corrective* SCOPF problems that include the possibility to optimally change control variables in post-contingency state (after the automatic reactions happened).

[☆] This paper consolidates and extends results presented in the conference paper [1].

Email addresses: maxime.velay@cea.fr / maxime.velay@g2elab.grenoble-inp.fr (M. Velay), meritxell.vinyals@cea.fr (M. Vinyals), yvon.besanger@g2elab.grenoble-inp.fr (Y. Besanger), nicolas.retiere@univ-grenoble-alpes.fr (N. Retiere)

[0] Institute of Engineering Univ. Grenoble Alpes

[1] A contingency here is defined as the set of system components that get disconnected (i.e. out-of-service) as a result of the propagation of the disturbance or of the initial contingency event itself.

[2] The response is governed by the speed droop of generators.

[3] The primary control reacts within the first seconds after the disturbance.

Due to the quadratic and sinusoidal relations between voltage magnitude and phase angle, and, active and reactive powers, SCOPF is a non-convex problem. To simplify the calculation, the AC power flow equations are often relaxed or approximated. In particular, in this paper, we use the linearized (DC) power flow approximation which neglects the losses on power lines and assumes constant voltage and small voltage phase angles. The DC approximation is used for N-1 calculations in today's power system industry due to its computational speed and simplicity [6, 7] with respect to the full AC power flow model. For example, DC-solutions are usually coupled with an AC feasibility check module in an iterative process towards obtaining solutions feasible to the AC power flow model.

Power systems are connected to their neighbours (e.g. 36 countries interconnected in Europe, forming the pan-European power system) to achieve better overall reliability and economical efficiency, via energy and reserve sharing between markets. These advantages are, yet, subject to have an effective cooperation and coordination among the interconnected TSOs and hence, not surprisingly, regional cooperation is at the core of the regional strategy of European TSOs for the decades to come [8]. Despite this fact, European regional coordination initiatives are in their early stages and most TSOs are still solving the SCOPF problem with limited coordination with their neighbours.

One of the main challenges to realize such inter-regional coordination is that the implementation of centralized approaches is undesirable, if not impossible, due to the technical difficulties for building (i.e. communication requirements for gathering data for the whole system) and solving (i.e. the high computational complexity) such interconnected problems of unprecedented scale. In addition to this, the centralization of inter-regional data is unlikely to be practical because TSOs may not be willing to disclose actual sensitive data (e.g. financial information, system topology and/or control regulations) to other TSOs. Also interoperability issues can arise from the use of different modeling and optimization tools by the different TSOs.

In view of the scalability, privacy and interoperability challenges, distributed optimization methods are gaining popularity [9]. Under distributed approaches, the large-scale power system is decomposed, usually based on Lagrangian decompositions, into smaller sub-regions whose problems are efficiently solved and coordinated to obtain the global optimal solution.

In more detail, Lagrangian relaxation performs this decomposition by deriving the Lagrangian dual problem, i.e. relaxing coupling constraints and introducing splitting variables [10, 11]. However, Lagrangian relaxation methods typically suffer from significant iteration oscillation leading to slow convergence. Augmented Lagrangian decomposition overcomes the poor convergence of conventional Lagrangian relaxation by introducing a quadratic penalty term to the objective function. This, unfortunately, comes with the price of destroying the separable structure of dual decomposition. The Alternating Direction Method of Multipliers (ADMM) [12] overcomes such limitations by combining the decomposability of standard dual decomposition with the superior convergence of the augmented Lagrangian methods. In more detail, ADMM can be viewed as a version of the method of multipliers in which separable minimization steps over different primal variables are performed in successive alternating steps, instead of the usual joint minimization. ADMM-based methods have been applied to solve the augmented Lagrangian decompositions of a wide variety of large-scale power system optimization problems [13, 14, 15, 16, 17, 18, 19, 20, 21, 22, 23], including the SCOPF problem [24, 25, 26], in a fully distributed manner. However, none of the above-cited works takes into account the automatic primary frequency control (PFC) of generators.

Against this background, this paper extends the distributed framework in [24] in order to take into account the automatic PFC of generators. By doing so, we are able to model contingencies states in DC-SCOPF involving a modification of the active power balance. Since in PFC, generators automatically adapt their production with respect to the frequency deviation and frequency deviation reflects the power balance across the whole power system, modeling it in a distributed manner is not a trivial task. In this paper, we provide the first totally distributed solution to this challenge through consensus optimization in conjunction with the ADMM algorithm.

More specifically, the main contributions of this work are:

- We extend the DC-SCOPF formulation from [24] by: 1) introducing a new variable representing the frequency deviation, computed by distributed consensus and used to coordinate the power reallocation process after an incident; 2) enhancing the local problem of each generator to consider how it adjusts its production after a contingency following its primary frequency regulation curve.
- We solve this problem in a distributed fashion via ADMM showing not only how the resulting algorithm can find a solution robust to the loss of generators but also how it can model contingencies states that lead to area separation (the contingency separates the network into two or more sub-networks). In particular, our algorithm is able to find a solution that in case of such contingency will lead to a stable operating point in each of the disconnected areas.
- We evaluate our approach on several standard IEEE systems to demonstrate its effectiveness and its capacity to deal with the disconnection of areas in interconnected systems.

The rest of this paper is structured as follows. Section 2 provides a review of the related literature whereas Section 3 gives some background on the decentralized SCOPF formulation, the ADMM algorithm and the primary frequency control scheme. Section 4 formulates the distributed SCOPF model with PFC and the derived ADMM distributed updates. Results on several standard IEEE test systems are presented in Section 5. Finally, Section 6 summarizes conclusions and plans for future research.

2. Related work

The main challenges and techniques to be addressed for solving SCOPF problems are reviewed in [2]. One of the ma-

jor issue comes from the high dimensionality of these problems [27, 2, 28], in comparison with the classic OPF due to the number of scenarios to consider. The dimension of the SCOPF problem is even larger when considering interconnected power systems. Several approaches have been implemented to deal with this issue, such as reducing the number of scenarios to consider [27] or the dimension itself by simplifying or omitting less affected regions of the system as in [29]. It is also possible to employ parallelization techniques that can speed up the solutions like the Benders decomposition scheme in [30]. Nonetheless, in interconnected systems, different actors are involved and need privacy for some sensitive or strategic data which makes more complicated such centralized approaches.

Distributed methods bring a solution to both interconnected problems by parallelizing the solution, and by limiting the sensitivity and the spreading of the data exchanged. Related work on distributed optimization for power system operation can be found in [9] and the references cited therein. Based on the type of information being exchanged, [9] divides the distributed methodologies applied in power system operation into two categories: (i) generator-based decomposition with price / cost information exchange and (ii) geography-based decomposition with physical information exchange. Generator-based decomposition approaches [31, 32] may lead to the exposure of the actors strategy (through price / cost information), and in addition, these methods have only proven to be efficient when neglecting global constraints of the system [9], e.g. power flow equations and capacity limits of transmission lines. Conversely, geography-based decomposition methods exchange information related to the physical measures (i.e. voltage and power flows) and provide a decomposition structure consistent with the topology of physical power systems (i.e. the large system is divided into several geographical sub-regions coupled by lines). Under this category, ADMM has been identified as one of the most applicable and efficient decomposition methods due to its simplicity and better convergence performance compared to other state-of-the-art algorithms for distributed optimization [12]. ADMM has been applied to OPF problems [33, 16, 22, 13, 23, 14, 15], and more recently, to SCOPF problems [24, 25, 34].

Due to the non-convex nature of AC power flow equations, ADMM is only assured to converge to the optimal solution under specific contexts, e.g., radial distribution networks [33]. Nonetheless, several works have reported good results when applying ADMM directly to non-convex AC-OPF problems: [16] showed how it converges to near-optimal solutions in a timely fashion relative to other models, while [22] reports convergence to a locally optimal solution on a large-scale Polish 2383-bus transmission system. To overcome the difficulty of solving non-convex OPF in a distributed manner, other works have opted for relaxing or approximating the AC power flows. For instance, several approaches proposed convexifying the OPF problem before applying the ADMM algorithm. Such convex relaxations include a semi-definitive program [13], sequential convex approximations [23] and second-order cone relaxations [14]. For a DC-OPF linearized approximation, Kraning *et al.* [15] suggested a methodology for decomposing the OPF problem among a collaborative agent network and a fully-distributed ADMM-based algorithm to solve it. The convergence criterion is provided and simulation results on large random meshed systems are conducted. More recently, some reports [35, 36] investigated the performance of ADMM for solving OPF problems with respect to different decomposition granularity (i.e. varying from tens to thousands of sub-regions), showing that the decomposition strategy seem to be a defining factor for the convergence speed. However, despite of testing the scalability of ADMM for large-scale power systems, all these above references address the OPF problem (i.e. without security constraints).

Several decentralized algorithms have been developed for solving the SCOPF problem considering only transmission contingencies and without modeling the PFC. [37] presents an agent-based fully distributed DC-SCOPF approach to model line failures but the optimization method capitalizes on the Lagrange Multipliers, which has poorer convergence and requires stronger conditions than the ADMM method used in this paper. In the current power system literature we also identify some papers employing ADMM to solve the SCOPF problem in a decentralized way. Chakrabarti *et al.* [24], building on the work of [15], were the first to apply ADMM to solve the preventive DC-SC-OPF problem with transmission line contingencies, handling different reliability constraints across multiple scenarios. However, the paper lacks any empirical evaluation in real circuits (e.g. the distributed algorithm is only evaluated in a single two bus system). In [34], authors employ ADMM with convergence acceleration strategies but to solve a corrective DC-SCOPF formulation without PFC that minimizes the number of post-contingency corrections and power rescheduled. Authors in [25] apply ADMM as an heuristic method to solve the AC-SCOPF problem (i.e. with the original AC equations) with line contingencies and test it in the large-scale Polish 3012-bus system. Results show how the ADMM algorithm is capable of yielding a robust solution, which is numerically proved to be the global optimum. Li *et al.* tackled, in [26], a corrective contingency-constrained tie-line scheduling problem, in the context of multi-area system, using a robust optimization formulation and the ADMM algorithm. The contingencies considered are, however, intra-area only, i.e. a contingency can only impact devices in its own region and they don't consider contingencies on tie-lines, while it can be very harmful.
Although all these cited studies solve a SCOPF problem via the ADMM algorithm, they neglect the action of the primary frequency control, and hence, these works do not integrate the real automatic reaction of the system to the loss of power balance.

In fact, as mentioned in [38], the primary frequency control is usually less studied than the other frequency controls in the literature. And yet, Karoui et al. [39] presents the modeling of the primary reserve allocation in the corrective SCOPF problem. However, the paper uses a centralized approach (i.e. the interior point method). Primary frequency control is also modeled and solved with a centralized iterative algorithm in [40], but its focus is on the optimization of the droop coefficients of the generators participating in the PFC.

In summary, while some centralized approaches account for the primary frequency control, it is not the case for existing de-

centralized approaches. Hence, this work is the first to propose a distributed security constrained optimal power flow with primary frequency control, using ADMM as a distributed algorithm and a subsequent implementation solved by distributed agents. As a result we are able to consider contingencies generating power imbalance, and specifically, on generators.

3. Background

In this section, we first review the ADMM algorithm and its application to the SCOPF problem (for further details we refer the readers to [24] and [15]). We then provide a formal definition of the primary frequency control scheme in power systems and some notation used in the rest of the paper.

3.1. Application of the ADMM to SCOPF problem

Following the network model proposed by Kraning et al. [15], we divide the set of power system network components into two groups: (i) the set of *nets* (N), that, similarly to the electrical bus concept, connect devices; and (ii) the set of *devices* (D), that is composed of all power components that are not buses. Each of these components $c \in N \cup D$ is associated to: (i) a local objective function that represents the component operating cost ($f_c(\cdot)$); and (ii) a set of constraints that the operation should satisfy in order to be feasible (C_c). We consider here the linearized, or DC, power flow equations and thus consider two types of variables: the active power and the voltage phase angle.

Now, we create an edge for every pair of components whose objective function or constraints have some variables in common (i.e. the cost and/or the feasibility of both components depend on at least some shared variables). We will refer to this set of edges as *terminals* (T).

For each component $c \in N \cup D$, we use c to refer to both the component itself as well as to the set of terminals associated with it, i.e., we say $t \in c$ if terminal t is associated with component c. As shown in [15], for a power network this leads to a bipartite graph between nets and devices in which each terminal t connects a device and a net. In other words, the sets of devices D and the set of nets N are both partitions of T, or, the other way round, the set of terminals T can be partitioned by either the devices or the nets. For example, Fig. 1a shows a simple 3-bus circuit whereas Fig. 1b shows its network model where nets are represented by rectangles, devices by circles and the terminals by lines.

This model is extended in [24] to solve a SCOPF problem in which the optimization is performed over a set of possible contingency scenarios, $\mathcal{L} = \{(0), \ldots, (|\mathcal{L}|)\}$. Here we assume that the first scenario, (0), is the one that stands for the base case (with no contingency). Given a scenario $(s) \in \mathcal{L}$ we define $D^{(s)}$ as the set of devices that are disconnected in that scenario.

Thus, in a SCOPF problem, each terminal $t \in T$ has associated one (active) power schedule over the set of contingencies $\mathcal{L}$: $p_t = (p_t^{(0)}, \ldots, p_t^{(|\mathcal{L}|)}) \in \mathbb{R}^{|\mathcal{L}|}$. For the rest of the paper we will follow the following sign convention: power coming out of a terminal to the device is positive and going into a terminal from the device is negative (for a net point of view, signs are inverted). Then, for all $(s) \in \mathcal{L}$, $p_t^{(s)}$ is the (real) power consumed (if positive, otherwise produced) by device d through terminal t, for the contingency scenario (s). We provide, in Fig. 1b, the nets and the devices partitions of the active power schedule of T to illustrate the partitioning of the set of terminals. Similarly, we use an analogous notation for voltage phase angle schedule over the set of contingencies $\theta_t = (\theta_t^{(0)}, \ldots, \theta_t^{(|\mathcal{L}|)}) \in \mathbb{R}^{|\mathcal{L}|}$.

The set of all power schedules associated with a component $c \in D \cup N$ (being c either a device or a net) is denoted by $p_c = \{p_t | t \in c\}$, which we can associate with a $|c| \times |\mathcal{L}|$ matrix. For example, in Fig. 1b the set of active power schedules of the device component l_{12} and of the net component n_2 are defined as $p_{l_{12}} = \{p_{t_2}, p_{t_3}\}$ and $p_{n_2} = \{p_{t_1}, p_{t_2}\}$ respectively. For voltage phase angle schedules we use an identical notation to power schedules, i.e. $\theta_c = \{\theta_t | t \in c\}$. Similarly, the set of all power schedules of the network is denoted by $p = \{p_t | t \in T\}$ and the set of all voltage phase angle schedules of the network by $\theta = \{\theta_t | t \in T\}$, each of which can be associated with a $|T| \times |\mathcal{L}|$ matrix.

Under this model, the global objective function of the SCOPF problem can be written as:

$$\begin{aligned} \min_{p,\theta \in \mathbb{R}^{|T| \times |\mathcal{L}|}} & \sum_{d \in D} f_d(p_d, \theta_d) + \sum_{n \in N} f_n(p_n, \theta_n) \\ \text{subject to } & \forall d \in D : p_d, \theta_d \in C_d, \\ & \forall n \in N : \; p_n, \theta_n \in C_n \end{aligned} \tag{1}$$

where (p_d, θ_d) and (p_n, θ_n) are the variables of p and θ respectively involved in f_d and in f_n.

The global objective function is intended to find the active power and voltage phase angle schedules that minimize the overall operating cost while satisfying the power flow equations and being feasible for all specified contingency scenarios.

Following [15, 24], this optimization problem can be solved by a distributed coordination protocol based on the Alternating Direction Method of Multipliers (ADMM) [12]. Under ADMM formulation, first, the nets objective functions are defined over a duplicated copy of the original variables (i.e. denoted as $\dot{p}$, $\dot{\theta}$) and equality coupling constraints ($p = \dot{p}$, $\theta = \dot{\theta}$) are added to keep the equivalence with Eq. 1.

$$\begin{aligned} \min_{p,\theta \in \mathbb{R}^{|T| \times |\mathcal{L}|}} & \sum_{d \in D} f_d(p_d, \theta_d) + \sum_{n \in N} f_n(\dot{p}_n, \dot{\theta}_n) \\ \text{subject to } & \forall d \in D : p_d, \theta_d \in C_d, \\ & \forall n \in N : \; \dot{p}_n, \dot{\theta}_n \in C_n, \\ & p = \dot{p}, \;\; \theta = \dot{\theta} \end{aligned} \tag{2}$$

The scaled form of the augmented Lagrangian is then formed by relaxing the equality coupling constraints:

$$\begin{aligned} L(p, \dot{p}, \theta, \dot{\theta}, u, v) = & \sum_{d \in D} f_d(p_d, \theta_d) + \sum_{n \in N} f_n(\dot{p}_n, \dot{\theta}_n) \\ & + \frac{\rho}{2}(||p - \dot{p} + u||_2^2 + ||\theta - \dot{\theta} + v||_2^2) \end{aligned} \tag{3}$$

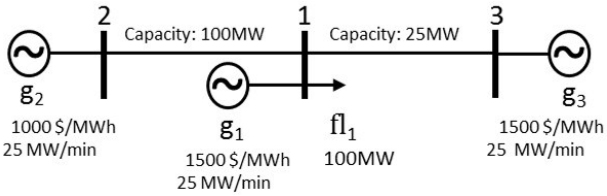

(a) 3-bus circuit

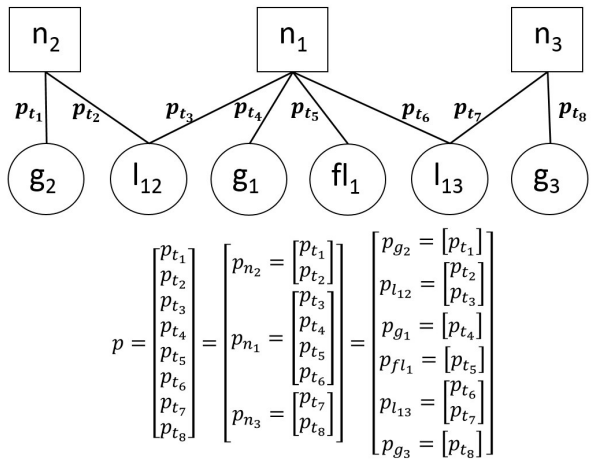

(b) Network model

Figure 1: a) A simple bus test circuit and b) its graphical representation in the network model from [15] and the partitions of the active power schedule.

where ρ is the scaling parameter, u and v are the dual variables associated, respectively, with the active power schedule p and the voltage phase angle schedule θ.

The problems then become separable using the fact that the set of devices D and the set of nets N are both partitions of the set of terminals T, and that imply the later equalities:

$$
\begin{aligned}
||p - \dot{p} + u||_2^2 &= \sum_{t \in T} ||p_t - \dot{p}_t + u_t||_2^2 \\
&= \sum_{d \in D} ||p_d - \dot{p}_d + u_d||_2^2 = \sum_{n \in N} ||p_n - \dot{p}_n + u_n||_2^2 \\
||\theta - \dot{\theta} + v||_2^2 &= \sum_{t \in T} ||\theta_t - \dot{\theta}_t + v_t||_2^2 \\
&= \sum_{d \in D} ||\theta_d - \dot{\theta}_d + v_d||_2^2 = \sum_{n \in N} ||\theta_n - \dot{\theta}_n + v_n||_2^2
\end{aligned}
$$

The ADMM algorithm eventually consists in, alternatively, minimizing the Lagrangian of Eq. 3, using previous equalities, by: first fixing the values of nets variables ($\dot{p}$, $\dot{\theta}$), second fixing the value of devices variables (p, θ), and finally updating the scaled dual variables (u and v). In that way, ADMM can be viewed as a version of the method of multipliers in which separable minimization steps over different primal variables are performed in successive steps. The convergence speed of ADMM depends on the choice of the scaling parameter (ρ) so in practice this parameter is tuned empirically for each specific application.

In a nutshell, the ADMM algorithm consists in iteratively applying the following three steps at a given iteration $k+1$ and for some scaling parameter $\rho > 0$:

The *device-minimization* step (i.e. parallelized among devices):

$$
\begin{aligned}
(p_d^{k+1}, \theta_d^{k+1}) = \arg \min_{p_d, \theta_d \in C_d} (f_d(p_d, \theta_d) + \\
\frac{\rho}{2}||p_d - \dot{p}_d^k + u_d^k||_2^2 + \frac{\rho}{2}||\theta_d - \dot{\theta}_d^k + v_d^k||_2^2), \ \ \forall d \in D
\end{aligned}
\tag{4}
$$

The *net-minimization* step (i.e. parallelized among nets):

$$
\begin{aligned}
(\dot{p}_n^{k+1}, \dot{\theta}_n^{k+1}) = \arg \min_{\dot{p}_n, \dot{\theta}_n \in C_n} (f_n(\dot{p}_n, \dot{\theta}_n) + \\
\frac{\rho}{2}||p_n^{k+1} - \dot{p}_n + u_n^k||_2^2 + \frac{\rho}{2}||\theta_n^{k+1} - \dot{\theta}_n + v_n^k||_2^2), \ \ \forall n \in N
\end{aligned}
\tag{5}
$$

The (price) *scaled dual variables* update (i.e. parallelized among nets):

$$
u_n^{k+1} = u_n^k + (p_n^{k+1} - \dot{p}_n^{k+1}), \ \ \forall n \in N \tag{6}
$$

$$
v_n^{k+1} = v_n^k + (\theta_n^{k+1} - \dot{\theta}_n^{k+1}), \ \ \forall n \in N \tag{7}
$$

The problem is, by construction, already separated in local sub-problems which allows each component (either net or device) to solve its sub-problem in parallel and to coordinate via message-passing through terminals.

At each iteration, each device component computes a minimization step for its local objective function (Eq. 4) that minimizes the operating cost of the device (i.e. encoded by f_d and C_d), and a penalty that depends on messages passed to it through its terminals by its neighboring nets in the previous iteration ($\dot{p}_n^k$, $\dot{\theta}_n^k$, u_n^k and v_n^k). Similarly, each net component computes its minimization (Eq. 5) and scaled dual variables steps (Eq. 6 and 7) with an argument that depends on messages passed to it through its terminals by its neighboring devices in the previous iteration (p_d^{k+1}, θ_d^{k+1}). In more detail, nets are loss-less energy carriers (i.e. buses) with zero cost function (e.g. $f_n(\cdot) = 0$) but with constraints on the power and phase schedules of their terminals that enforce Kirchhoff's physical laws. Following [15, 24] each net $n \in N$ requires *power balance* and *phase consistency*, which is represented by the constraints:

$$
\sum_{t \in n} \dot{p}_t = 0, \tag{8}
$$

$$
\dot{\theta}_t = \dot{\theta}_{t'}, \ \ \forall t, t' \in n \tag{9}
$$

For these constraints specified above the computation of the *net-minimization* step (Eq. 5) can be solved analytically as in [15][4] as follows, $\forall (s) \in \mathcal{L}, \ \ \forall t \in n$:

$$
\dot{p}_t^{k+1(s)} = p_t^{k+1(s)} - \frac{1}{|n|} \sum_{t \in n} p_t^{k+1(s)}, \tag{10}
$$

$$
\dot{\theta}_t^{k+1(s)} = \frac{1}{|n|} \sum_{t \in n} \theta_t^{k+1(s)}, \tag{11}
$$

with $|n|$ the number of terminals (connections) of net n, i.e. the size of vectors $\dot{p}_n$ and $\dot{\theta}_n$.

[4] Eq. 10 and 11 are the results of a projection on an hyperplane defined by the constraints of Eq. 8 and 9.

These three steps are done iteratively until a sufficient consistency is reached at each net. The consistency is quantified using primal and dual residuals, and the threshold for the convergence depends on the required absolute tolerance (ϵ^{abs}). ADMM is guaranteed to converge to the optimal solution when all devices have convex, closed, proper objective functions and a feasible solution to the SCOPF exists.

3.2. Primary frequency control

In this section, the local steady-state equations of the PFC are first presented, before providing the global variables and calculations of the frequency deviation across the overall system. Since this paper focuses on preventive SCOPF, the change of generators power schedule, following a contingency $(s) \in \mathcal{L}$, is only due to the response of the power system automatic control:

$$\forall g, \quad p_g^{(s)} = p_g^{(0)} + \Delta p_g^{(s)} \tag{12}$$

where $p_g^{(s)}$ is the generation after PFC due to contingency (s) of generator g, $p_g^{(0)}$ is the generation in the base case (0), i.e. prior any contingency and $\Delta p_g^{(s)}$ is the primary frequency response of the generator g due to contingency (s).

The primary frequency response in steady-state follows the following five principles:

1. After the primary frequency response, the system should reach a new steady-state and thus the generation should equal the consumption. In other words, the power balance of the system should be kept after the primary frequency response of generators, despite the disturbance, ΔP, of the initial power balance of the system.
2. The primary frequency response of a generator g to a disturbance of the power balance of the system is determined by its coefficient K_g.[5] Formally:

$$\Delta p_g^{(s)} = K_g \cdot \alpha^{(s)} \tag{13}$$

where $\alpha^{(s)}$ is the steady-state relative frequency deviation for contingency $(s) \in \mathcal{L}$ defined as:

$$\alpha^{(s)} = -\frac{\Delta f}{f_0} = \frac{\Delta P}{\sum\limits_{g \notin D^{(s)}} K_g} \tag{14}$$

where f_0 is the base frequency[6], Δf is the frequency deviation after PFC and ΔP is the power deviation from schedule.
Although the relative frequency deviation is the same across the whole power system (i.e. it is a global value), notice that, in the case of contingencies leading to area separation, we will have a different frequency deviation for each separated area.

3. The active production of each generator has to remain within its production limits

$$P^{min} \leq p_g^{(s)} \leq P^{max} \tag{15}$$

4. The primary response of each generator cannot exceed the ramp constraints[7]:

$$R^{min} \leq \Delta p_g^{(s)} \leq R^{max} \tag{16}$$

5. Once a generator reaches its (ramp or production) limits, the other generators have to compensate the non-allocated power according to their own speed droop. Thus, when a generator does not change as expected because it reached some constraints, this is reflected in the frequency deviation $\Delta f^{(s)}$ and in the contribution of the other generators.

4. Distributed DC-SCOPF with PFC

In this section, we present our distributed algorithm to the DC-SCOPF problem. We extend the distributed (N-1) DC-SCOPF model reviewed in Section 3 in order to be able to take into account the automatic response of generators as part of its participation to the PFC. With this aim, we introduce a new variable representing the (steady-state) relative frequency deviation that will be used to coordinate the power allocation process after a contingency takes place. Since the frequency deviation for a contingency scenario is a global variable of the power system the SCOPF problem with PFC needs to be carefully reformulated into a suitable form so that it can be solved by ADMM in a distributed manner.

With this aim, we extend the SCOPF model in Section 3.1 by creating for each contingency scenario (s) a duplicated relative frequency deviation variable ($\alpha^{(s)}$) at each terminal. As a result, the objective function of the SCOPF problem (Eq. 2) is reformulated to include the relative frequency variables as:

$$\begin{aligned} \min_{p,\theta,\alpha \in \mathbb{R}^{|\mathcal{T}|\times|\mathcal{L}|}} & \sum_{d \in D} f_d(p_d, \theta_d, \alpha_d) + \sum_{n \in N} f_n(\dot{p}_n, \dot{\theta}_n, \dot{\alpha}_n) \\ \text{subject to } & \forall d \in D : p_d, \theta_d, \alpha_d \in C_d, \\ & \forall n \in N : \ \dot{p}_n, \dot{\theta}_n, \dot{\alpha}_n \in C_n, \\ & p = \dot{p}, \ \ \theta = \dot{\theta}, \ \ \alpha = \dot{\alpha} \end{aligned} \tag{17}$$

Thus, by duplicating relative frequency deviation variables, the problem decomposes into sub-problems as in the original model. The correct relative frequency deviation is obtained after the set of duplicated (local) variables related to the same contingency iteratively reaches consensus via ADMM. Moreover, the nets and devices sub-problems are modified to take into account the PFC as follows:

- *Nets:* in addition to the Kirchhoff's constraints, the net model is extended to also verify locally that, in each scenario, all the terminals have the same relative frequency deviation.

[5] K_g is defined as the ratio of the nominal active power and the speed droop of the generator (both constants and depending on the generators characteristics).

[6] Regulated frequency of the grid (50Hz or 60Hz depending of the country)

[7] $\Delta p_g^{(s)}$ is limited because generators cannot change their production at any speed.

- *Transmission lines:* the model is extended to restrict that local relative frequency deviations on both sides of the line are equal for each scenario.
- *Generators:* the model is reformulated so that its production on the different scenarios is proportional to the relative frequency deviation and to the generator coefficient, when the generator is not the device undergoing an outage. Since, as we will see, this formulation leads to a non-convex device-minimization problem, we propose an approximation to return to convexity.

The following sections detail this reformulation of nets (Section 4.1) and devices (Section 4.2) local problems.

4.1. Formulation of nets local sub-problem

In addition to the Kirchhoff's constraints, to consider primary frequency control, each net constrains that in each scenario all the terminals have the same relative frequency deviation:

$$\dot{\alpha}_t^{(s)} = \dot{\alpha}_{t'}^{(s)}, \ \ \forall t, t' \in n, \ \forall (s) \in \mathcal{L} \tag{18}$$

For these constraints on the relative frequency deviation the ADMM *net-minimization* step (Eq. 5) can be solved analytically (as a projection on an hyperplane, as in [15]) as follows:

$$\dot{\alpha}_t^{k+1(s)} = \frac{1}{|n|} \sum_{t \in n} \alpha_t^{k+1(s)} \tag{19}$$

For the power and phase angle variables, since they are constrained as defined in Eq. 8 and 9, they are updated by the same analytical solutions as in Eq. 10 and 11.

Moreover, in addition to the *scaled dual variables* updates related to the active power and voltage phase angle (Eq. 6-7), each net also updates the dual variables related to the relative frequency deviation variables:

$$\omega_n^{k+1} = \omega_n^k + (\alpha_n^{k+1} - \dot{\alpha}_n^{k+1}), \ \ \forall n \in N \tag{20}$$

4.2. Formulation of devices local sub-problems

Each device component is responsible for defining its local cost function and constraints as well as for implementing the *device-minimization* step. Formally, $\forall d \in D$:

$$\begin{aligned}(p_d^{k+1(s)}, \theta_d^{k+1(s)}, \alpha_d^{k+1(s)}) = \underset{p_d, \theta_d, \alpha_d \in C_d}{\arg\min} \ (f_d(p_d, \theta_d, \alpha_d) \\ + \frac{\rho}{2}(||p_d - \dot{p}_d^k + u_d^k||_2^2 + ||\theta_d - \dot{\theta}_d^k + v_d^k||_2^2 \\ + ||\alpha_d - \dot{\alpha}_d^k + w_d^k||_2^2)),\end{aligned} \tag{21}$$

The next subsections detail these local sub-problems and local optimizations steps for the three types of devices considered in this paper: generators, transmission lines and loads.

4.2.1. Generators

A generator is a single terminal device which produces power with a local cost for operating the generator at a given power level and some operating constraints that limit this power output. Following [15, 24] we consider that a generator g encodes its production cost by means of a quadratic cost function:

$$f_g(p_g^{(0)}) = \beta \cdot \left(p_g^{(0)}\right)^2 + \gamma \cdot p_g^{(0)} \tag{22}$$

where $\beta, \ \gamma > 0$ are respectively the quadratic and linear cost coefficients. It is observed here that as it is common in SCOPF problems, the cost of operation of the generation only depends on its power generation in the base case scenario (i.e. contingencies are not expected to happen in a regular basis so the cost of generation to deal with a contingency is usually neglected).

Also in the base case the power output of the generator is bounded by its production limits:

$$P_g^{min} \leq p_g^{(0)} \leq P_g^{max} \tag{23}$$

Then, for contingency cases implying the outage of the generator ($g \in D^{(s)}$), the power output of the generator g should be zero:

$$p_g^{(s)} = 0, \ \ \forall (s) \in \{\mathcal{L} | g \in D^{(s)}\} \tag{24}$$

Finally, for the rest of contingency cases (i.e. in which the generator is operative), we need to extend the set of constraints to take into account the generator automatic frequency response. Hence, unlike [24], the power output of the generator in these contingencies will not be the same as the output in the base case scenario but instead it will follow the generator automatic adaptation of the generation. This adaptation is proportional to the generator coefficient and bounded by its ramp limits, $\forall (s) \in \{\mathcal{L} | g \notin D^{(s)}\}$:

$$\Delta p_g^{(s)} = \begin{cases} -R_g^{min} & \text{if } K_g \cdot \alpha_g^{(s)} \leq -R_g^{min} \\ K_g \cdot \alpha_g^{(s)} & \text{if } -R_g^{min} \leq K_g \cdot \alpha_g^{(s)} \leq R_g^{max} \\ R_g^{max} & \text{if } K_g \cdot \alpha_g^{(s)} \geq R_g^{max} \end{cases} \tag{25}$$

Moreover, in all scenarios the power output of the generator has to remain within its production limits, $\forall (s) \in \{\mathcal{L} | g \notin D^{(s)}\}$:

$$p_g^{(s)} = \begin{cases} P_g^{min} & \text{if } p_g^{(0)} + \Delta p_g^{(s)} \leq P_g^{min} \\ p_g^{(0)} + \Delta p_g^{(s)} & \text{if } P_g^{min} \leq p_g^{(0)} + \Delta p_g^{(s)} \leq P_g^{max} \\ P_g^{max} & \text{if } p_g^{(0)} + \Delta p_g^{(s)} \geq P_g^{max} \end{cases} \tag{26}$$

Unfortunately, the step functions in Eq. 25 and Eq. 26 lead to a non-convex device-minimization problem. To overcome this, we fix the primary frequency response of each generator as $p_g^{(s)} = p_g^{(0)} + K_g \cdot \alpha_g^{(s)}$ and we replace the step functions by two linear constraints that directly bound the domain of variables $\alpha_g^{(s)}$ and $p_g^{(s)}$. In particular, Eq. 25 is replaced by:

$$\frac{-R_g^{min}}{K_g} \leq \alpha_g^{(s)} \leq \frac{R_g^{max}}{K_g} \tag{27}$$

and Eq. 26 by:

$$P_g^{min} \leq p_g^{(s)} \leq P_g^{max} \quad (28)$$

Such modifications allow us to keep the device-minimization problem for generators convex and thus, we can rely on off-the-shelf optimization tools to solve it efficiently. In particular, we solve the unconstrained problem and then project the solution on the intersection of the constraints defined by Eq. 27 and Eq. 28, using Dykstra's alternating projection algorithm [41].

Notice that these two constraints are more restrictive than the original ones (i.e. they reduce the feasible region of the problem). In more detail, with the original constraints it may be the case that the automatic frequency response of a generator reaches either its ramp or power outputs limits and that the other generators have, in turn, to compensate the non-allocated power according to their coefficient. Instead, the linear constraints do not consider this case and the model is restricted to find base case configurations that are capable to deal with any single-element contingency and in which the automatic response of generators do not reach their local limits (i.e. no compensation will be needed from any generator further than the planned one). We acknowledge that this more restrictive model can end up finding less economically efficient base case solutions. However, we also highlight that in such cases the relative frequency deviation corresponding to the power imbalance in some contingency will also be lower and hence, the solutions found under this model can be also seen as more secure.

4.2.2. Transmission lines

A (transmission) line is a two-terminal device used to transfer power from one net (i.e. bus) to another. Here, we use a linear DC-OPF model for lines, often used in the literature to get rid of the non-convexity of the physics of AC circuits. Under this model the power flow equations ignore real power losses as well as reactive power and voltage magnitude is assumed to be equal to 1 pu. A line l has a zero cost function ($f_l(\cdot) = 0$) but the power flows and voltage phase angles on both sides of the line are constrained. In particular, the power flow through the line depends on: (i) the power schedules (p_{l_1} and p_{l_2}) and voltage phase angles (θ_{l_1} and θ_{l_2}) at both sides of the line (i.e. indexes 1 and 2 refer to the two different sides of the line l); and on the susceptance of the line (b).

In particular, for contingency cases in which the line l is not involved in the outage (i.e. $\forall(s) \in \{\mathcal{L}|l \notin D^{(s)}\}$) the power and phase schedules should satisfy the relations:

$$p_{l_1}^{(s)} = -p_{l_2}^{(s)} = b \cdot (\theta_{l_2}^{(s)} - \theta_{l_1}^{(s)}), \quad (29)$$

But if the contingency case implies the outage of the line l (i.e. $\forall(s) \in \{\mathcal{L}|l \notin D^{(s)}\}$) the power transmitted through the line should be zero:

$$p_{l_1}^{(s)} = p_{l_2}^{(s)} = 0, \quad (30)$$

Moreover, in each scenario, the power going through the line has to be lower than its maximum capacity (i.e. long-term capacity in the base case and short-term capacity in a contingency case):

$$-C_l^{max} \leq p_{l_1}^{(s)} \leq C_l^{max}, \ \ \forall(s) \in \mathcal{L} \quad (31)$$

Finally, the line also constrains that the relative frequency deviation on both sides of the line are equal:

$$\alpha_{l_1}^{(s)} = \alpha_{l_2}^{(s)}, \ \forall(s) \in \{\mathcal{L}|l \notin D^{(s)}\} \quad (32)$$

Notice that the problem of transmission lines is separable over the set of scenarios (i.e. there is no constraint linking the variables of different scenarios) and hence line sub-problems can be solved independently for each scenario. Similarly, the terms depending on the relative frequency deviation variables for a given scenario are independent from other types of variables. Thus, given a scenario $(s) \in \{\mathcal{L}|l \notin D^{(s)}\}$ the device-minimization step to update the relative frequency deviation variables reduces to:

$$\begin{aligned}(\alpha_{l_1}^{k+1(s)}, \alpha_{l_2}^{k+1(s)}) = &\underset{\alpha_{l_1},\alpha_{l_2}}{\arg\min}(\frac{\rho}{2}||\alpha_{l_1} - \dot{\alpha}_{l_1}^{k(s)} + w_{l_1}^{k(s)}||_2^2 \\ &+ \frac{\rho}{2}||\alpha_{l_2} - \dot{\alpha}_{l_2}^{k(s)} + w_{l_2}^{k(s)}||_2^2) \\ &\text{subject to: } \alpha_{l_1}^{(s)} = \alpha_{l_2}^{(s)}\end{aligned} \quad (33)$$

Eq. 33 results in a projection on an hyperplane and can be solved analytically (see [42]) as follows:

$$\alpha_{l_1}^{k+1(s)} = \alpha_{l_2}^{k+1(s)} = \frac{\dot{\alpha}_{l_1}^{k(s)} - \omega_{l_1}^{k(s)} + \dot{\alpha}_{l_2}^{k(s)} - \omega_{l_2}^{k(s)}}{2} \quad (34)$$

The active power schedules and voltage phase angles are coupled in each contingency scenario, when on the contrary, the variables between the different scenarios are independent. Thus, given a scenario $(s) \in \{\mathcal{L}|l \notin D^{(s)}\}$ the transmission line problem to update the active power schedules and voltage phase angles variables reduces to:

$$\begin{aligned}(p_{l_1}^{k+1(s)}, \theta_{l_1}^{k+1(s)}, p_{l_2}^{k+1(s)}, \theta_{l_2}^{k+1(s)}) = &\underset{p_{l_1},\theta_{l_1},p_{l_2},\theta_{l_2}}{\arg\min} (\\ \frac{\rho}{2}||p_{l_1} - \dot{p}_{l_1}^{k(s)} + u_{l_1}^{k(s)}||_2^2 + \frac{\rho}{2}||p_{l_2} - \dot{p}_{l_2}^{k(s)} + u_{l_2}^{k(s)}||_2^2 \\ +\frac{\rho}{2}||\theta_{l_1} - \dot{\theta}_{l_1}^{k(s)} + v_{l_1}^{k(s)}||_2^2 + \frac{\rho}{2}||\theta_{l_2} - \dot{\theta}_{l_2}^{k(s)} + v_{l_2}^{k(s)}||_2^2) \\ \text{subject to : } p_{l_1} = b \cdot (\theta_{l_2} - \theta_{l_1}), \quad p_{l_1} = -p_{l_2}, \\ -C_l^{max} \leq p_{l_1} \leq C_l^{max}\end{aligned} \quad (35)$$

We solve the problem in Eq. 35 while ignoring the inequality constraints that model the line capacity, and by using a matrix formulation. We introduce the following vectors and matrix:

$X_{l_i}^{(s)} = \begin{bmatrix} p_{l_i}^{(s)} \\ \theta_{l_i}^{(s)} \end{bmatrix}$, $ZU_{l_i}^{k(s)} = \begin{bmatrix} \dot{p}_{l_i}^{k(s)} - u_{l_i}^{k(s)} \\ \dot{\theta}_{l_i}^{k(s)} - v_{l_i}^{k(s)} \end{bmatrix}$, and $B = \begin{bmatrix} -1 & 0 \\ \frac{1}{b} & 1 \end{bmatrix}$.

With i being equal either to 1 or 2 depending on the side l_1 or l_2 of the line. The solution is then the vector:

$$X_{l_1}^{k+1(s)} = (I + B^T \cdot B)^{-1} \left(ZU_{l_1}^{k(s)} + B^T \cdot ZU_{l_2}^{k(s)} \right) \quad (36)$$

When the capacity limit of the line is reached, the optimal active power is equal to the limit reached noted p_l^{lim} and the voltage phase angles are determined using Eq. 29 and the preferred value from each bus. Formally:

$\theta_{l_1} = \frac{1}{2} \cdot \left(\dot{\theta}_{l_1}^{k(s)} - v_{l_1}^{k(s)} + \dot{\theta}_{l_1}^{k(s)} - v_{l_1}^{k(s)} + \frac{p_l^{lim}}{b_l} \right)$,

$\theta_{l_2} = \frac{p_l^{lim}}{b_l} + \theta_{l_1}$.

All in all, the line sub-problems, represented by Eq. 33 and 35, are eventually solved analytically.

4.2.3. Fixed loads

A fixed load f_l is a single terminal device with zero cost function ($f_{fl}(\cdot) = 0$) which is simply described by a desired consumption $p_{f_l} \in \mathbb{R}$. In this paper, we assume that only generation will adapt in front of a contingency (i.e. loads will remain fixed) and hence, the solution for a fixed load remains constant across all iterations of the algorithm as $\forall(s) \in \{\mathcal{L}|f_l \notin D^{(s)}\}, p_{fl}^{(s)} = p_{f_l}$.

5. Simulation results

This section presents simulation results on three circuits: the IEEE 14-bus, the large-scale IEEE RTS 96 3-area system and a two-area system (derived from the duplication of the IEEE 9-bus). For each circuit, we compute the N-1 SCOPF with PFC solution with the ADMM-approach proposed in this paper as well as the OPF solution using the ADMM-approach from [15] for assessing the cost of security.[8] The distributed ADMM algorithm is implemented, in both cases, as a multi-agent system using the Java Agent Development (JADE) platform [43], where each agent solves its corresponding sub-problem in parallel. The two ADMM parameters (the scaling parameter and the absolute tolerance) are set to the values given in Table 1. The base power of the systems is 100MVA (used for per unit calculations), so for a tolerance of 10^{-4}, it means that at most the power balance needs to be respected with a tolerance of maximum 10kW.

	IEEE 14-bus	IEEE RTS 96 3-area	Two area system
ρ	1.0	0.1	1.0
ϵ	10^{-4}	10^{-3}	10^{-4}

Table 1: ADMM parameters values.

5.1. IEEE 14-bus

In this subsection the proposed SCOPF with PFC is tested on the IEEE-14-bus test system with the transmission data from the Power System Test Case Archive [9]. The system, represented in Figure 2, is composed of 11 loads, 20 lines and 5 generators. We completed the model by setting the line capacity limits to 110MW for both, short-term and long-term settings. Table 2 details the parameters used for the different generators. Notice that each generator is modeled with a ramp up limit of 35MW/min. Table 2 also specifies the generator coefficient K_g, computed as the ratio of the nominal active power of the generator, set to the generator maximum power output (P^{max}), and the speed droop, set to 5%.

Solving the OPF problem takes 1093 iterations whereas the SCOPF problem taking into account N-1 contingencies (of all lines and generators) is solved in 3582 iterations. Regarding the cost of security, the N-1 security constraints increases the cost of generation by 6.2% (i.e. from 7835$ for the OPF solution to 8359$ for the N-1 solution).

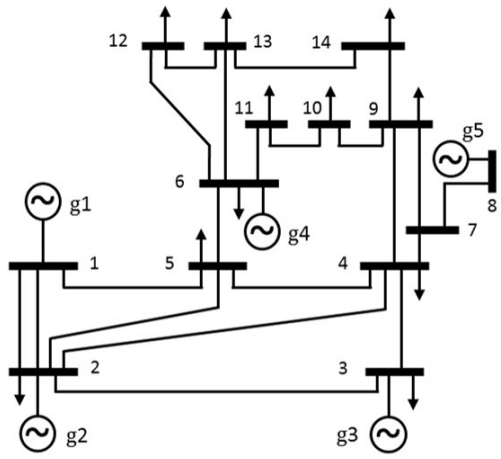

Figure 2: IEEE 14-bus test system.

Gen.	P^{max} MW	P^{min} MW	R^{max} MW/min	β \$/MWh^2	γ \$/MWh	K_g MW/%
$g1$	332.4	0	35	0.043	20	6.65
$g2$	140	0	35	0.25	20	2.80
$g3$	100	0	35	0.01	40	2.00
$g4$	100	0	35	0.01	40	2.00
$g5$	100	0	35	0.01	40	2.00

Table 2: Generators parameters used in the IEEE 14-bus test system.

The largest frequency deviation is reached in the contingency case that models the disconnection of generator g1, that as stated in Table 2 is the cheapest and largest generator of the system. Table 3 shows that in this case, the frequency deviation of the system computed by our algorithm corresponds to 1.25% deviation, i.e. 625 mHz for a 50Hz system. It is easy to see that this value corresponds to the theoretical frequency deviation value: in the base case, generator g_1 supplies 110MW (see Table 3), so $\Delta P = 100MW$ when this generator is out of service, and then by Eq. 14, we obtain $\alpha = 110MW/(K_{g_2} + K_{g_3} + K_{g_4} + K_{g_5}) = 1.25\%$ using the coefficients of generators from Table 2.

Next we detail the constraints involved in this test case to further illustrate the ability of the method to enforce some global constraints, in a fully distributed manner, and the impact of the assumption taken in the generators model. Since g_2 has the largest coefficient K_g when g_1 is disconnected and all generators have the same ramp capacity, g_2 is the limiting generator in term of relative frequency deviation of the system. The power supply of generator g_1 in the base case ($p_{g_1}^{(0)}$) is then constrained by Eq. 27, so that, its disconnection does not cause a relative frequency deviation greater than $\frac{R^{max}}{K_{g_2}} = 1.25\%$. This explains why the active power schedule of g_1, in Table 3, decreased by 35%, from 168MW in the OPF solution to 110MW in the SCOPF solution.

[8] The cost of security is defined as the percentage cost increase between the solution of the OPF problem and that of the SCOPF.

[9] https://www2.ee.washington.edu/research/pstca/

		SCOPF contingency scenarios	
Variable	OPF	base case	g1
$\alpha^{(s)}$	–	–	1.25 %
p_{g1}	-168 MW	-110 MW	0 MW
p_{g2}	-43.3 MW	-41.5 MW	-76.5 MW
p_{g3}	-42.9 MW	-36.3 MW	-61.3 MW
p_{g4}	0 MW	-36.3 MW	-61.3 MW
p_{g5}	-4.7 MW	-35 MW	-60 MW

Table 3: Comparison of the results between OPF and N-1 SCOPF for the IEEE 14-bus test system.

5.2. Application to a large-scale system: IEEE RTS 96 3-area

This subsection investigates the scalability of our algorithm by testing it on a larger system with a larger number of contingencies: the IEEE RTS 96 3-area test system [44]. The problem leads to 340 different sub-problems when counting the buses, lines, loads and generators, each managed by a different agent.

In the experiments, we considered three sets of contingencies: (1) all single-line contingencies; (2) all single-generator contingencies; and (3) all single-line and single-generator contingencies. These three sets allow a comparison of the impact of the number of scenarios on the number of iterations needed by the algorithm to converge.

Table 4 provides a summary of the number of contingency scenarios considered in each test, the number of iterations needed, and the costs of operation. The cost of the OPF solution is 167k$ when the cost of the N-1 SCOPF with PFC when considering all contingencies (lines and generators) is 179k$ which makes a 7% increase to guarantee the security of the system. Observe that the cost of security mainly comes from the contingencies on generators as when considering only lines failures, the solution of the SCOPF does not increase the cost of operation and so the base case solution in this case is the same as the one of the OPF.

The largest relative frequency deviation is of 0.18% deviation, i.e. 90mHz for a 50Hz system, and is obtained when any of the six generators producing the maximum output in the base case (385.5MW) is disconnected.

Notice that the SCOPF solution needed 35% less iterations to converge compared to the OPF solution. A plausible explanation for this finding is that by adding more constraints, the feasible solution space is reduced, and thus, it is easier to explore [45]. Thus, as other works (e.g. [36]) found that considering a larger circuit in OPF does not necessarily imply a worse convergence performance, here our results show that considering a larger number of scenarios in SCOPF does not necessarily imply a worse convergence performance either.

5.3. Separation of transmission system areas in a two-area system

In this subsection, we investigate the capability of our model to consider the disconnection of two interconnected transmission areas. With this purpose, we built a two-area system (in Figure 3) by duplicating the IEEE 9-bus test system and adding an interconnection line (i.e. between bus 7 and bus 16) with a capacity of 250MW connecting both systems. Table 5 details the parameters used for the different generators. Notice that the power exchange between both areas is ensured by multiplying the quadratic and linear cost coefficient of generation by 10 in the second area (buses 10 to 18). Also, all generators have the same ramp up equal to 60MW/min. Finally, the maximum power output of generators of the second area is reduced by 100MW and the load on bus 16 is increased by 30MW to make the two areas consumptions different.

	# of scenarios	# of iterations	Cost k$
OPF	0	7627	167.3
Lines contingencies	120	6778	167.3
Generators contingencies	96	3881	179.0
All lines and generators	216	4947	179.7

Table 4: Results on the IEEE RTS 96 3-area test system.

Gen.	P^{max} MW	P^{min} MW	R^{max} MW/min	β \$/MWh^2	γ \$/MWh	K_g MW/%
$g1$	250	0	60	0.11	5	5.0
$g2$	300	0	60	0.085	1.2	6.0
$g3$	270	0	60	0.1225	1	5.4
$g4$	150	0	60	1.1	50	3.0
$g5$	200	0	60	1.0	12	4.0
$g6$	170	0	60	1.3	10	3.4

Table 5: Generator parameters in the IEEE 9-bus duplicated test system.

We first solve the OPF problem on this system and, as expected, the power flow through the interconnection line 7-16 reaches its maximum, i.e. 250MW, with a generation cost of 19.9k$. It took 1357 iterations to find the solution.

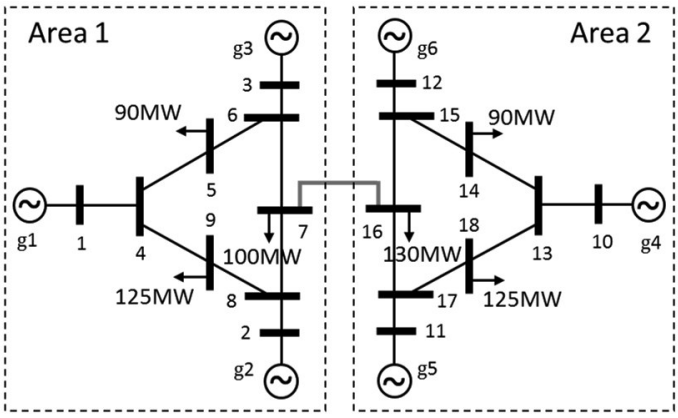

Figure 3: Two area test system derived from the duplication of the IEEE 9-bus test system.

We then consider the SCOPF with only one contingency: the disconnection of line 7-16 which leads to the separation of the two areas. Note that under this contingency, the primary reserves of each area will need to recover from the lost interconnection line power transfer and hence the maximum power transfer capacity of this line in SCOPF cannot exceed the reserve of any of the two areas. We can compute the primary

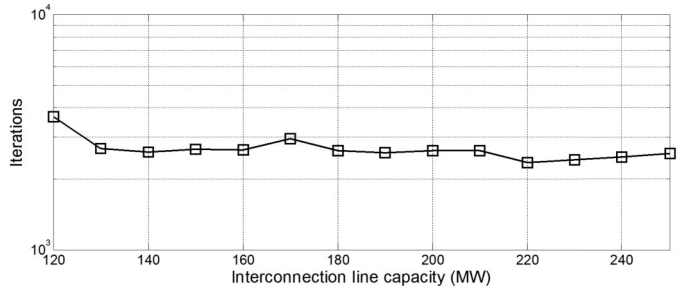

(a) Number of iterations to reach convergence.

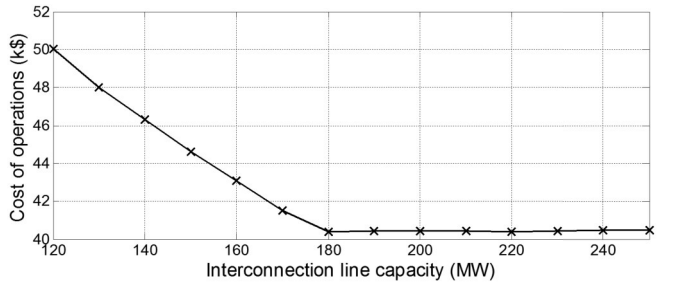

(b) Cost of the N-1 solution.

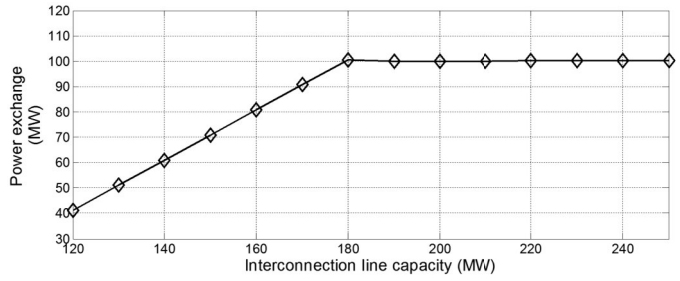

(c) Power exchanged in the tie line.

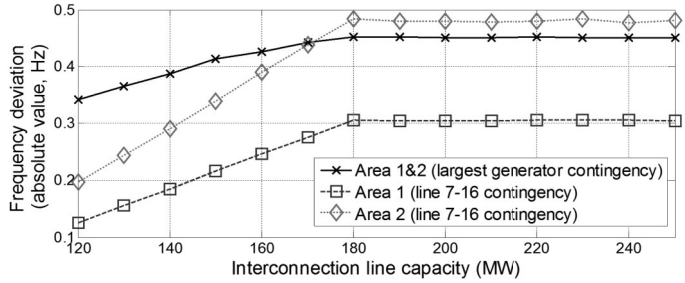

(d) Largest frequency deviation resulting from a generator disconnection and absolute frequency deviation value in each area in case of separation (line 7-16 contingency).

Figure 4: Duplicated IEEE 9-bus results.

reserves of each area based on the maximum value of α that is constrained as in Eq. 27. The most restrictive area is the second area with a maximum relative frequency deviation of $\alpha = 1.5\%$. This corresponds to the maximum primary reserves in this area and to a maximum power transfer in the tie line of 156MW and to a relative frequency deviation for the first area of $\alpha = -0.95\%$. These values are the same than the ones obtained by our algorithm. The SCOPF solution in this case has a 43.5% increment in cost with respect to the OPF solution (i.e. to 28.6k$) explained by the increment of the cost of generation parameters in the second area. The solution was found in 1913 iterations.

Most of the algorithms solving SCOPF problem do not consider the separation of a system into different areas, mainly because, to be able to consider those cases, further developments are needed, such as the detection of the separated areas. A major advantage of our approach is that there is neither need to detect the separation of the system, nor to adapt the algorithm to consider the separation scheme.

After this first test, we propose to consider all single-lines and single-generators contingencies, and to vary the capacity limit of line 7-16 to evaluate how having a less or more constrained problem affects the cost of the solution. Figure 4a depicts the number of iterations needed to find the N-1 solution by the SCOPF with PFC when varying the capacity of the interconnection line among the two areas. The proposed distributed algorithm is able to find the N-1 solution for all the scenarios and the security constraints do not impact significantly the number of iterations needed to reach the convergence criteria. This instantiates the good scalability of the algorithm, even when considering the separation of the system into different areas.

Figure 4b depicts the cost of the N-1 solution when varying the capacity of the interconnection line among the two areas. Observe that as expected, when increasing the tie line capacity, the cost of the solutions decreases. However, after reaching a capacity of 180MW, the cost does not vary, which means that the capacity of line 7-16 is no longer the limiting constraint. This hypothesis is confirmed in Figure 4c where we see that, indeed, reducing the capacity of line 7-16 decreases the power exchange and thus tends to distribute the power generation in the two areas. The maximum power exchange in these two regions is then 100MW, regardless of the capacity of interconnection if it is greater than 180MW. Finally, Figure 4d shows the largest frequency deviation that results from a generator disconnection, as well as, the absolute value of the relative frequency deviation that results from the disconnection of line 7-16, in each area. The objective here is to assess if the separation is more disturbing than the loss of any of the generators, and how it evolves when the transfer capacity of the interconnection line changes. We observe that for a capacity up to 170MW, the worst deviation is caused by the loss of a generator. In contrast, with a capacity greater than 170WM, the event that would provoke the worst frequency deviation is the loss of the interconnection line. In summary, experiments show that the proposed algorithm is able to integrate the separation of an interconnected system, and to propose a schedule that allows a safe separation.

6. Conclusions and future work

This paper presents the first totally distributed ADMM-based method to solve the security constrained power flow with primary frequency control. In more detail, we extend the distributed security-constrained optimal power flow framework from [24] to take into account the automatic primary frequency control of generators and we solve it in a fully distributed manner

using the ADMM algorithm. The contribution of this paper allows to distributedly find solutions for the SCOPF problem that remain stable after the disconnection of a generator, a line or even after system area separation – all without requiring any form of central coordination. Moreover, the distributivity of the method naturally preserves the independence of individual region operators and achieves high scalability while fully taking advantage of their interconnection via a localized peer-to-peer communication paradigm.

Empirical results on the IEEE 14-bus and the IEEE 3-area RTS 96 tests systems show how our method is able to find optimal SCOPF solutions for these circuits, defining for each contingency case the corresponding power flows and steady-state frequency deviation. These results demonstrate not only the high scalability of our approach but also that considering a larger number of contingencies does not necessarily implies a worse convergence performance (solving the SCOPF problem in a large multi-area system, with 216 contingencies, takes 35% less iterations than solving the OPF problem). We finally tested the robustness of our distributed method to the most disturbing change in an interconnected power system, that is the separation of areas of the system. Results obtained on a duplicated IEEE 9-bus test system eventually prove the intrinsic robustness of this method to any change of topology without even any need of propagate the origin of the change.

References

[1] M. Velay, M. Vinyals, Y. Besanger, N. Retière, Agent-based security constrained optimal power flow with primary frequency control, in: EUMAS 2017 - Proceedings of the Fifteen European Workshop on Multi-Agent Systems, Évry, France, December 14-15, 2017, 2017, p. To appear.

[2] F. Capitanescu, J. M. Ramos, P. Panciatici, D. Kirschen, A. M. Marcolini, L. Platbrood, L. Wehenkel, State-of-the-art, challenges, and future trends in security constrained optimal power flow, Electric Power Systems Research 81 (8) (2011) 1731–1741.

[3] M. Huneault, F. D. Galiana, A survey of the optimal power flow literature, IEEE Transactions on Power Systems 6 (2) (1991) 762–770.

[4] A. Pinar, J. Meza, V. Donde, B. Lesieutre, Optimization strategies for the vulnerability analysis of the electric power grid, SIAM Journal on Optimization 20 (4) (2010) 1786–1810.

[5] M. Eremia, M. Shahidehpour, Handbook of electrical power system dynamics: modeling, stability, and control, Vol. 92, John Wiley & Sons, 2013.

[6] R. P. ONeill, T. Dautel, E. Krall, Recent iso software enhancements and future software and modeling plans, Federal Energy Regulatory Commission, Washington, DC, Tech. Rep.

[7] Q. Wang, J. D. McCalley, T. Zheng, E. Litvinov, A computational strategy to solve preventive risk-based security-constrained opf, IEEE Transactions on Power Systems 28 (2) (2013) 1666–1675.

[8] ENTSO-Es, Where the energy union starts: regions, https://www.entsoe.eu/Documents/Publications/vision/entsoe_vision04_regions_web.pdf (November 2015).

[9] Y. Wang, S. Wang, L. Wu, Distributed optimization approaches for emerging power systems operation : A review, Electric Power Systems Research 144 (2017) 127–135.

[10] A. J. Conejo, J. A. Aguado, Multi-area coordinated decentralized dc optimal power flow, IEEE Transactions on Power Systems 13 (4) (1998) 1272–1278. doi:10.1109/59.736264.

[11] A. Y. S. Lam, B. Zhang, D. N. C. Tse, Distributed algorithms for optimal power flow problem, in: Proceedings of the 51th IEEE Conference on Decision and Control, CDC 2012, December 10-13, 2012, Maui, HI, USA, 2012, pp. 430–437.

[12] S. Boyd, N. Parikh, E. Chu, B. Peleato, J. Eckstein, Distributed Optimization and Statistical Learning via the Alternating Direction Method of Multipliers, Foundations and Trends in Machine Learning 3 (1) (2011) 1–122.

[13] E. Dall'Anese, H. Zhu, G. B. Giannakis, Distributed optimal power flow for smart microgrids, IEEE Transactions on Smart Grid 4 (3) (2013) 1464–1475. doi:10.1109/TSG.2013.2248175.

[14] Q. Peng, S. H. Low, Distributed algorithm for optimal power flow on a radial network, in: 53rd IEEE Conference on Decision and Control, 2014, pp. 167–172. doi:10.1109/CDC.2014.7039376.

[15] M. Kraning, E. Chu, J. Lavaei, S. P. Boyd, Dynamic network energy management via proximal message passing, Foundations and Trends in Optimization 1 (2) (2014) 73–126.

[16] P. Scott, S. Thiébaux, Distributed multi-period optimal power flow for demand response in microgrids, in: Proceedings of the 2015 ACM Sixth International Conference on Future Energy Systems, e-Energy 2015, Bangalore, India, July 14-17, 2015, 2015, pp. 17–26.

[17] M. Mazidi, A. Zakariazadeh, S. Jadid, P. Siano, Integrated scheduling of renewable generation and demand response programs in a microgrid, Energy Conversion and Management 86 (Supplement C) (2014) 1118 – 1127.

[18] E. Loukarakis, C. J. Dent, J. W. Bialek, Decentralized multi-period economic dispatch for real-time flexible demand management, IEEE Transactions on Power Systems 31 (1) (2016) 672–684.

[19] W. Zheng, W. Wu, B. Zhang, H. Sun, Y. Liu, A fully distributed reactive power optimization and control method for active distribution networks, IEEE Transactions on Smart Grid 7 (2) (2016) 1021–1033. doi:10.1109/TSG.2015.2396493.

[20] B. A. Robbins, A. D. Domínguez-García, Optimal reactive power dispatch for voltage regulation in unbalanced distribution systems, IEEE Transactions on Power Systems 31 (4) (2016) 2903–2913.

[21] M. Vinyals, M. Velay, M. Sisinni, A multi-agent system for energy trading between prosumers, in: 14th International Conference on Distributed Computing and Artificial Intelligence (DCAI'17), 2017, pp. 79–86.

[22] J. Guo, G. Hug, O. K. Tonguz, Enabling distributed optimization in large-scale power systems, CoRR abs/1605.09785. arXiv:1605.09785.

[23] S. Magnússon, P. C. Weeraddana, C. Fischione, A distributed approach for the optimal power-flow problem based on admm and sequential convex approximations, IEEE Transactions on Control of Network Systems 2 (3) (2015) 238–253.

[24] S. Chakrabarti, M. Kraning, E. Chu, R. Baldick, S. Boyd, Security Constrained Optimal Power Flow via proximal message passing, 2014 Clemson University Power Systems Conference (2014) 1–8.

[25] D. Phan, J. Kalagnanam, Some efficient optimization methods for solving the security-constrained optimal power flow problem, IEEE Transactions on Power Systems 29 (2) (2014) 863–872. doi:10.1109/TPWRS.2013.2283175.

[26] Z. Li, W. Wu, B. Zeng, M. Shahidehpour, B. Zhang, Decentralized Contingency-Constrained Tie-Line Scheduling for Multi-Area Power Grids, IEEE Transactions on Power Systems (2016) 1–14doi:10.1109/TPWRS.2016.2539278.

[27] F. Capitanescu, L. Wehenkel, A new iterative approach to the corrective security-constrained optimal power flow problem, IEEE transactions on power systems 23 (4) (2008) 1533–1541.

[28] Q. Wang, J. D. McCalley, T. Zheng, E. Litvinov, Solving corrective risk-based security-constrained optimal power flow with lagrangian relaxation and benders decomposition, International Journal of Electrical Power & Energy Systems 75 (2016) 255–264.

[29] F. Karbalaei, H. Shahbazi, M. Mahdavi, A new method for solving preventive security-constrained optimal power flow based on linear network compression, International Journal of Electrical Power & Energy Systems 96 (2018) 23–29.

[30] A. Monticelli, M. V. F. Pereira, S. Granville, Security-constrained optimal power flow with post-contigency corrective rescheduling, IEEE Transactions on Power Systems 2 (1) (1987) 175–180.

[31] Z. Zhang, M.-Y. Chow, Convergence analysis of the incremental cost consensus algorithm under different communication network topologies in a smart grid, IEEE Transactions on power systems 27 (2012) 1761–1768.

[32] W. T. Elsayed, E. F. El-Saadany, A fully decentralized approach for solving the economic dispatch problem, IEEE Transactions on Power Systems 30 (4) (2015) 2179–2189.

[33] A. X. Sun, D. T. Phan, S. Ghosh, Fully decentralized ac optimal power flow algorithms, in: 2013 IEEE Power Energy Society General Meeting, 2013, pp. 1–5. doi:10.1109/PESMG.2013.6672864.
[34] D. T. Phan, X. A. Sun, Minimal impact corrective actions in security-constrained optimal power flow via sparsity regularization, IEEE Transactions on Power Systems 30 (4) (2015) 1947–1956.
[35] Y. Wang, L. Wu, S. Wang, A fully-decentralized consensus-based admm approach for dc-opf with demand response, IEEE Transactions on Smart Grid 8 (6) (2017) 2637–2647.
[36] E. Loukarakis, J. W. Bialek, C. J. Dent, Investigation of maximum possible opf problem decomposition degree for decentralized energy markets, IEEE Transactions on Power Systems 30 (5) (2015) 2566–2578.
[37] J. Mohammadi, G. Hug, S. Kar, Agent-based distributed security constrained optimal power flow, IEEE Transactions on Smart Grid PP (99) (2016) 1–1.
[38] M. Chertkov, Y. Dvorkin, Chance constrained optimal power flow with primary frequency response, arXiv preprint arXiv:1703.06724.
[39] K. Karoui, H. Crisciu, L. Platbrood, Modeling the primary reserve allocation in preventive and curative security constrained opf, in: Transmission and Distribution Conference and Exposition, 2010 IEEE PES, IEEE, 2010, pp. 1–6.
[40] Y. Dvorkin, P. Henneaux, D. S. Kirschen, H. Pandi, Optimizing primary response in preventive security-constrained optimal power flow, IEEE Systems Journal PP (99) (2016) 1–10.
[41] J. P. Boyle, R. L. Dykstra, A method for finding projections onto the intersection of convex sets in hilbert spaces, in: Advances in order restricted statistical inference, Springer, 1986, pp. 28–47.
[42] N. Parikh, S. Boyd, et al., Proximal algorithms, Foundations and Trends® in Optimization 1 (3) (2014) 127–239.
[43] F. Bellifemine, F. Bergenti, G. Caire, A. Poggi, JADE - A java agent development framework, in: Multi-Agent Programming: Languages, Platforms and Applications, 2005, pp. 125–147.
[44] R. T. Force, The ieee reliability test system-1996, IEEE Trans. Power Syst 14 (3) (1999) 1010–1020.
[45] M. Yokoo, Why adding more constraints makes a problem easier for hill-climbing algorithms: Analyzing landscapes of csps, in: Proceedings of the 3rd International Conference on Principles and Practice of Constraint Programming, CP'97, Springer-Verlag, Berlin, Heidelberg, 1997, pp. 356–370. doi:10.1007/BFb0017451.
URL https://doi.org/10.1007/BFb0017451